Since January 2020 Elsevier has created a COVID-19 resource centre with free information in English and Mandarin on the novel coronavirus COVID-19. The COVID-19 resource centre is hosted on Elsevier Connect, the company's public news and information website.

Virology 550 (2020) 78–88

Contents lists available at ScienceDirect

Virology

journal homepage: www.elsevier.com/locate/virology

Host cell p53 associates with the feline calicivirus major viral capsid protein VP1, the protease-polymerase NS6/7, and the double-stranded RNA playing a role in virus replication

Adrian Trujillo-Uscanga, Ana Lorena Gutiérrez-Escolano*

Departamento de Infectómica y Patogénesis Molecular, Centro de Investigación y de Estudios Avanzados del IPN, México City, Mexico

ARTICLE INFO

Keywords:
Feline calicivirus
p53
VP1
dsRNA
Protease-polymerase NS6/7
RNA-protein interaction
Replication complexes

ABSTRACT

p53 is implicated in several cellular pathways such as induction of cell-cycle arrest, differentiation, senescence, and apoptosis. p53 is activated by a broad range of stress signals, including viral infections. While some viruses activate p53, others induce its inactivation, and occasionally p53 is differentially modulated during the replicative cycle. During calicivirus infections, apoptosis is required for virus exit and spread into the host; yet, the role of p53 during infection is unknown. By confocal microscopy, we found that p53 associates with FCV VP1, the protease-polymerase NS6/7, and the dsRNA. This interaction was further confirmed by proximity ligation assays, suggesting that p53 participates in the FCV replication. Knocked-down of p53 expression in CrFK cells before infection, resulted in a strong reduction of the non-structural protein levels and a decrease of the viral progeny production. These results indicate that p53 is associated with the viral replication complex and is required for an efficient FCV replication.

1. Introduction

Feline Calicivirus (FCV) belongs to the *Vesivirus* genus of the *Caliciviridae* family, which currently comprises eleven genera containing viruses that infect a wide range of vertebrates (Vinjé et al., 2019). Caliciviruses have a single-stranded, positive-sense RNA genome (gRNA) of 6.4–8.5 kilobases (kb) in length, which is covalently attached to the viral protein genome-linked (VPg) in its 5' end and is polyadenylated. FCV genomic RNA (gRNA) is composed of 3 open reading frames (ORFs). The expression of the ORF1 results in a polyprotein that is processed by the viral protease-polymerase, the non-structural protein (NS) 6/7, to generate the six non-structural viral proteins (NS1-NS6/7). Both ORF 2 and 3 encode for the structural proteins; the ORF2 gives rise to the precursor of the major capsid protein VP1, which is further cleaved by the NS6/7 protease-polymerase to generate the leader of the capsid (LC) protein and the mature VP1, whereas the ORF3 encodes for the minor capsid protein VP2 necessary to produce infectious viral particles (Herbert et al., 1996) (S. V. Sosnovtsev, Belliot, Chang, Onwudiwe and Green, 2005); both VP1 and VP2 are translated from a subgenomic RNA (sgRNA).

FCV uses the Junctional Adhesion Molecule 1 (f-JAM1) as its functional receptor (Makino et al., 2006), enters its target cells through clathrin-mediated endocytosis (Stuart and Brown, 2006) followed by the release of the genomic RNA into the cytosol where it is immediately translated to produce the NS proteins, essential for the replication complexes (RCs) formation (Bailey et al., 2010). RCs are membranous-derived compartments where the synthesis of both the gRNA and the sgRNA occurs. Once synthesized, the sgRNA is promptly translated to produce the structural proteins; therefore, these membranous components contain high amounts of viral RNA and proteins, being VP1 the most abundant viral protein (Green et al., 2002). FCV viral capsid is composed of 90 dimers of VP1 and a few copies of VP2. Both structural proteins are assembled concomitantly with the gRNA to form the viral progeny, which exits the infected cells by apoptosis (Stanislav V. Sosnovtsev, Prikhod'ko, Belliot, Cohen and Green, 2003) (Barrera-Vázquez et al., 2019).

Apoptosis is a highly regulated process essential for the establishment of the calicivirus immunopathogenic phenotype, particularly to facilitate virus dissemination in the host [Reviewed in: (Peñaflor-téllez, Trujillo-uscanga, Escobar-almazán, & Gutiérrez-escolano, 2019)]. Moreover, recent evidence indicates that apoptosis is a mechanism to suppress the translation of induced interferon-stimulated genes (ISG) to impair the host innate immune response to norovirus infection (Emmott et al., 2017).

* Corresponding author. Departamento de Infectómica y Patogénesis Molecular, Centro de Investigación y de Estudios Avanzados del IPN, Av. IPN 2508. Col. San Pedro Zacatenco, CDMX, C.P. 07360, Mexico.
E-mail address: alonso@cinvestav.mx (A.L. Gutiérrez-Escolano).

https://doi.org/10.1016/j.virol.2020.08.008
Received 15 April 2020; Received in revised form 12 August 2020; Accepted 18 August 2020
Available online 27 August 2020
0042-6822/

One of the most important cell factors involved in apoptosis induction is the Tumor Protein p53 (p53), a 393 amino acid protein expressed from the *TP53* gene (Saha et al., 2015), also known as the "guardian of the genome" that functions as a DNA sequence-specific transcriptional regulator. p53 controls various cellular pathways such as cell cycle arrest at the G1/S regulation point on DNA damage recognition, differentiation, and senescence by activating DNA repair proteins when the DNA has sustained damage, and apoptosis when DNA damage is irreparable [Reviewed in: (Aloni-Grinstein et al., 2018) (Mishra and Laboratories, 2015)]. One of the most important proteins activated by p53 is the Cyclin-dependent kinase (CDK) inhibitor1 (p21), implicated in the progression of the cell cycle, transcription regulation, and apoptosis (Karimian et al., 2016). p21 is considered as an indicator of p53 activity (Georgakilas et al., 2017).

p53 exists in an inactive state in normal cells due to its interaction with its negative regulator, the mouse double-minute-2 homolog (MDM2) protein (Momand et al., 1992); however, DNA damage produced by cell stress conditions induces its dissociation and the further activation of p53 by its accumulation, posttranslational modifications, and conformational changes [Reviewed in: (Kastenhuber and Lowe, 2017)]. On activation, p53 may induce cell-cycle arrest for DNA repair, or may induce apoptosis to eliminate the altered cells; however, what determines p53 to stimulate one pathway or the other is still a matter of investigation [Reviewed in: (Kastenhuber and Lowe, 2017)]. As p53 is activated by several and varied stress signals, it is not surprising that virus-infected cells harbor altered p53 functions to achieve successful replication and spread throughout the host [Reviewed in: (Sato and Tsurumi, 2013) (Aloni-Grinstein et al., 2018)].

Viruses modulate p53 functions in different manners: single-stranded RNA viruses such as the human coronavirus NL63 (HCoV-NL63) induces its degradation of p53 (Yuan et al., 2015) to ensure viral growth in infected cells (Ma-Lauer et al., 2016), Zika (ZIKV) and West Nile (WNV) activate p53 to facilitate their replication (El Ghouzzi et al., 2016) (Teng et al., 2017) (Yang et al., 2008) while Adenovirus (ADV), Vaccinia virus (VACV), Tanapox virus (TPV) and Human papillomavirus (HPV) all DNA viruses, inhibit p53 activity. Moreover, some other viruses such as the simian virus 40 (SV40), the Human immunodeficiency virus (HIV), and Herpex simplex virus (HSV) activate and inhibit p53 in a stage-specific manner [Reviewed in: (Aloni-Grinstein et al., 2018)].

Even though p53 is implicated in the induction of apoptosis and in many viral infections, its role during calicivirus infection has not been studied. Here we found that p53 interacts with FCV dsRNA, the protease-polymerase NS6/7, and VP1 in the RC; moreover, knockdown of p53 resulted in a significant reduction of the NS viral protein synthesis and virus production, indicating its role for efficient viral replication.

2. Materials and methods

Cells and virus infection. The Crandell Feline Kidney (CrFK) cells (Crandell et al., 1973) obtained from the American Type Culture Collection (ATCC) (Rockville, MD) were grown in Eagle's minimal essential medium with Earle's balanced salt solution and 2 mM L-glutamine that was modified by the ATCC to contain 1.0 mM sodium pyruvate, 0.1 mM nonessential amino acids, 1.5 g/l sodium bicarbonate. The medium was supplemented with 10% bovine fetal serum, 5000 U of penicillin, and 5 μg/ml of streptomycin. Cells were grown in a 5% CO_2 incubator at 37 °C (Santos-Valencia et al., 2019). The FCV Urbana strain was obtained by the reverse genetic system using the pQ14 infectious clone (Sosnovtsev and Green, 1995). Virus titers were determined by plaque assay as previously described (Escobar-Herrera et al., 2007).

Western Blot assays. Mock and FCV infected cells with FCV at an multiplicity of infection (MOI) of 5 were washed with phosphate buffer saline (PBS), lysed in NP40 lysis buffer (150 mM NaCl; 1% NP40, Tris pH 8) and boiled for 10 min. Forty μg of total protein cell extracts were analyzed by SDS-PAGE and transferred to a 0.22 μm nitrocellulose membranes. The membranes were blocked with 5% skimmed milk in Tris-buffered saline (500 mM Tris, 50 mM NaCl) in 0.05% Tween (TBS-T) for 30 min at room temperature (RT) and incubated overnight at 4 °C with the following antibodies: mouse *anti*-p53 (Sc-374,087, Santa Cruz Biotechnology) in a 1:500 dilution in TBS-T-5% skimmed milk; rabbit *anti*-P21 (Sc-397, Santa Cruz Biotechnology); rabbit *anti*-FCV NS6/7 (Kindly donated by Ian Goodfellow) diluted in a 1:10,000 PBS-5% skimmed milk; and mouse *anti*-Annexin A2 (AnxA2) used as previously reported (Santos-Valencia et al., 2019). The membranes were washed with 0.05% TBS-T and incubated 2 h with the appropriate anti-rabbit-HRP or anti-mouse-HRP secondary antibodies diluted in 1:10,000 PBS-5% skimmed milk at RT and developed using chemiluminescence (PIERCsE). Quantification of protein levels was achieved by measuring band intensities in the scanned images using ImageJ software (http://rsb.info.nih.gov/ij) and expressed as relative expression units.

Far Western blot assay. *Homo sapiens* p53 wild type recombinant protein was obtained by electroelution from the *E. coli* BL21 (DE3) pLysS strain prokaryotic system using the pET15b vector [Human p53 (1–393), Cat. 24,859, Addgene]. Feline calicivirus VP1 Urbana strain recombinant protein was obtained from the pGEX-VP1 expression vector (Paredes-Morales et al.; unpublished data). Total protein extracts from mock-infected and infected cells were transferred to a 0.22 μm nitrocellulose membrane as previously described, blocked with PBS-5% skimmed milk for 2 h at RT, incubated with 10 μg of each recombinant protein for 4 h at RT, and washed three times with PBS for 10 min. The anti-His (1:5000) and the anti-mouse-HRP antibodies (1:10,000) were used to detect His-p53 protein. *Anti*-GST-HRP (1:500) antibody was used to detect FCV VP1-GST.

Pull-down assay. The FCV Urbana strain VP1 protein was cloned into the pGex-5X expression vector (FCV-VP1-GST) (Paredes-Morales et al., unpublished data). The *Escherichia coli* BL-21 strain was transformed with 1 μg of the FCV VP1-GST expression vector and grown to OD_{600} of 0.6, and protein expression was induced by 0.5 mM of Isopropyl β-D-1-thiogalactopyranoside (IPTG) for 4 h at 37 °C gently shaken. The recombinant protein was purified by electroelution for 1 h at 120 V. Mock-infected CrFK protein cell lysates (600 μg) were incubated with 50 μl of glutathione-agarose beads for 2 h at 4°Cwith gentle shaking. The mixture was centrifuged at 14,000 rpm for 5 min at 4 °C, and the supernatant was recovered, mixed with 50 μl of glutathione-agarose beads and 10 μg of the recombinant VP1-GST protein and incubated 2 h at 4°Cwith gentle shaking. The mixture was centrifuged at 14,000 rpm at 4 °C, and the beads were washed three times with cold PBS and eluted with 20 mM reduced glutathione-50 mM Tris-HCl (pH 8), and centrifuged at 14,000 rpm at 4°CTheelutedproductswereanalyzedbywesternblotting using the corresponding antibodies. Forty μg of GST protein (corresponding to an equimolar amount of VP1-GST protein) was used as a negative control.

Overlay assays. To determine the direct interaction between p53 and VP1, 5 μg of VP1-GST or GST were subjected by SDS-PAGE and transferred to a nitrocellulose membrane. The membrane was blocked as was mentioned before and incubated with 10 μg of p53-His in PBS-5% skimmed milk for 2 h at RT. After three washes with PBS, the anti-His antibody was incubated (ON) at 4 °C in gentle shaking. The secondary anti-mouse antibody was diluted (1:10,000) in PBS-5% milk. The interaction was analyzed by chemiluminescence.

siRNA–mediated knockdown of p53. For the siRNA-mediated knockdown of p53 expression, transfections were carried out as previously described (Cancio-Lonches et al., 2011). Briefly, CrFK cells were plated in a 24-well plate to reach 80% confluence. After 24 h, 200 nM of the non-targeting-siRNA (QIAGEN) or p53-siRNAs (QIAGEN) and 2.5 μl lipofectamine were mixed separately with 100 μl Opti-MEM, respectively for 10 min at RT. The two mixtures were combined, incubated at RT for 10 min, and then diluted in 100 μl Opti-MEM. The mixture was added directly to the cells, and transfection with the siRNAs was carried out at 37 °C for 8 h, followed by the addition of 200 μl growth medium and additional incubation for 24 h. After transfection, cells were

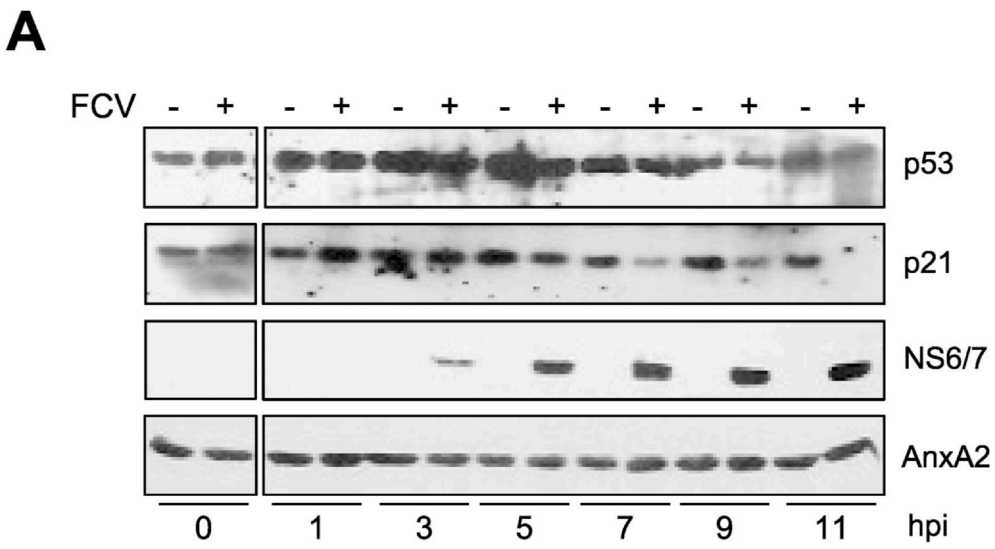

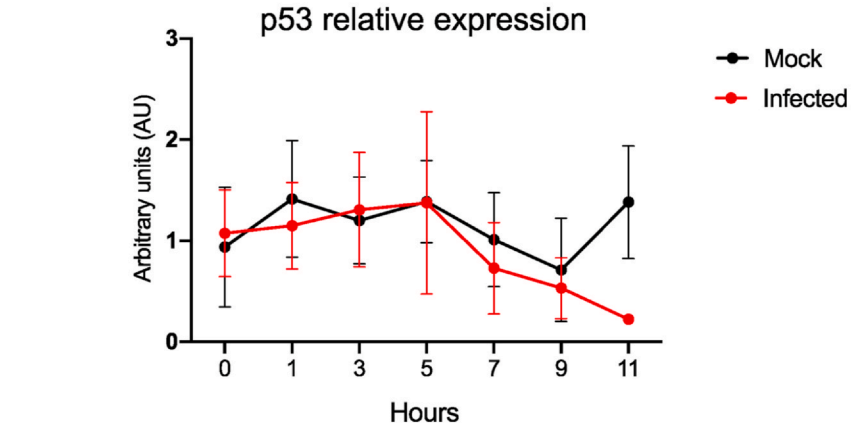

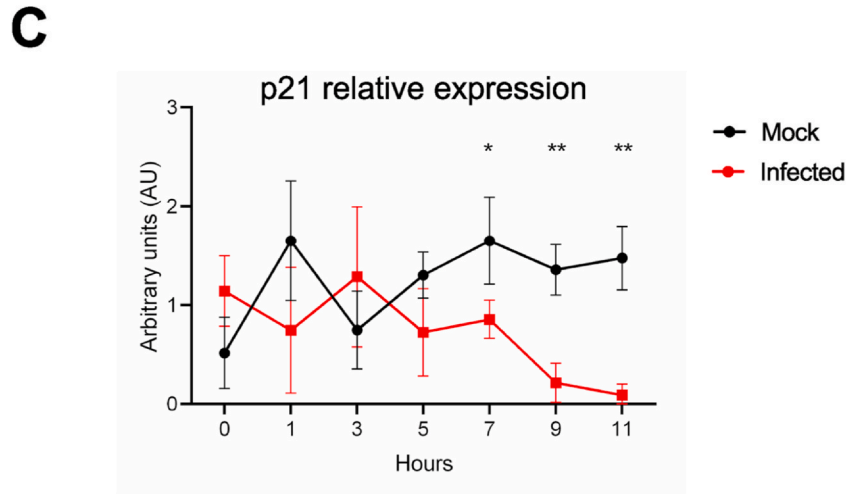

Fig. 1. p53 expression during FCV infection. A) Total protein extracts from mock-infected (−) or FCV infected (+) CrFK cells at an MOI of 5, were obtained at 0, 1, 3, 5, 7, 9, and 11 h and subjected to SDS-PAGE. Protein expression was analyzed by western blotting using specific antibodies. NS6/7 indicates virus infection; AnxA2 was used as the loading control. B) p53, and C) p21 band intensities of scanned images were quantified using ImageJ software and expressed as relative expression. Standard deviations were obtained from at least 3 independent assays. Values of $p \leq 0.05$ (*) and ≤ 0.0001 (**), calculated by two-way ANOVA using GraphPad Prism 8.00 software, are indicated.

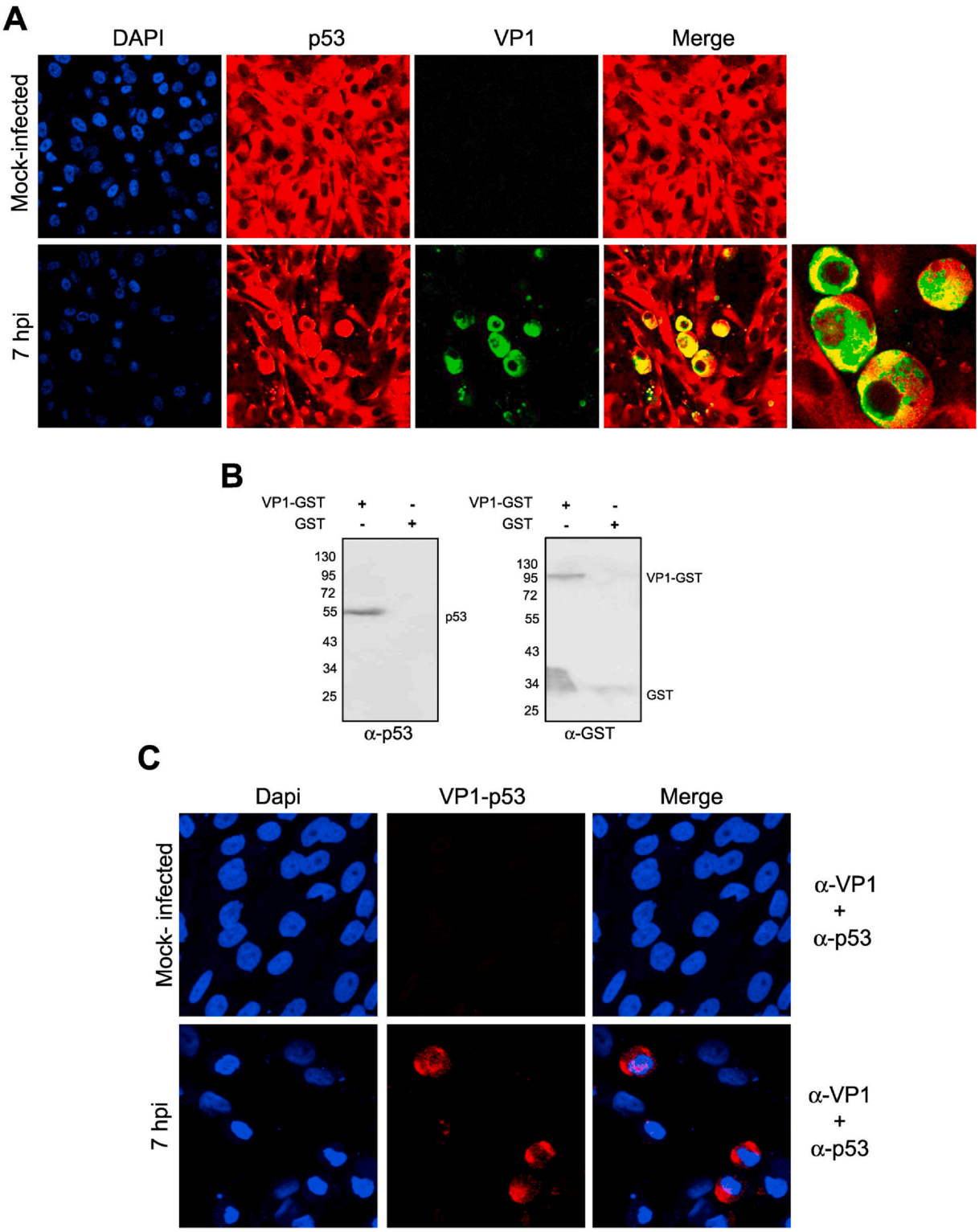

Fig. 2. p53 interacts with FCV VP1 in *in vitro* assays and during FCV infection. A) Monolayers of mock-infected or FCV CrFK cells were infected at an MOI of 5 for 7 h, and immunostained with an *anti*-p53 (red), and *anti*-VP1 (green) antibodies, followed by Alexa Fluor 594 (red) and Alexa Fluor 488 (green) respectively. DAPI was used for nuclear (blue) staining. The cells were examined in a Zeiss LSM 700 confocal microscope. Images correspond to a z-stack of 15 slices and are representative of three independent experiments. Merged and zoom images are indicated. Colocalization rates of p53 and VP1 at 7hpi (0.65 ± 0.11) were calculated by Pearson's coefficient correlation using the Icy software (http://icy.bioimageanalysis.org). B) Recombinant FCV VP1-GST or GST proteins coupled to glutathione-agarose beads were incubated with total mock-infected protein extracts. After several washes, the eluted proteins were analyzed for the presence of p53 by western blotting using *anti*-p53 and *anti*-GST antibodies. C) Proximity ligation assay (PLA-Duolink) between VP1 and p53 in FCV infected cells at 7 h. PLA signals (red) represent dual-recognition against p53 and VP1. DAPI was used for nuclear (blue) staining. The cells were examined in a Zeiss LSM 700 confocal microscope.

infected with FCV at an multiplicity of infection (MOI) of 5, and at 5 and 7 hpi were lysed with Laemmli 1X buffer. The levels of the p53, viral protease-polymerase NS6/7, and Glyceraldehyde 3-phosphate dehydrogenase (GAPDH) or annexin A2 (AnxA2) proteins were determined by Western blotting.

Cell viability and proliferation assays. Cells were seeded in 96-well plates and were untreated, mock-transfected or transfected with 200 nM of the non-targeting-siRNA or 100 and 200 nM of the p53-siRNA for 24 h. The viability of the cells was measured with the Cell Titer 96 AQueous nonradioactive cell proliferation assay according to the manufacturer's instructions (MTS assay, G3580, Promega). The viable cells were normalized in relation to the control cells. Cell proliferation was measured by counting the number of cells after 24 h of transfection with both siRNAs. We selected the cells with fibroblast phenotype with a Nikon Eclipse Ti–U microscope; the number of cells was obtained with the NIS-Elements AR analysis software, and compared in three different fields under both transfection conditions.

Immunofluorescence assays. CrFK cells were plated on glass coverslips and infected or not with FCV at an MOI of 5 at the indicated times. After infection, the cells were treated with cytoskeleton buffer (MES 10 mM; NaCl 50 mM; EGTA 0.5 M; $MgCl_2$ 1 M; Glucose 5 mM; pH 6.1) for 5 min. Monolayers were fixed with a 0.03 gr/ml PBS-paraformaldehyde (PFA) solution for 20 min at RT, washed three times with PBS for 5 min, permeabilized in a 0.002% PFA-Triton X 100 solution for 20 min at RT, and washed three times with PBS. The cells were blocked with 0.5% porcine skin gelatin (Sigma) in PBS for 40 min at RT, washed three times with PBS and incubated at 4ºC with the corresponding antibody: rabbit *anti*-p53 (Sc-6243, Santa Cruz Biotechnology) (1:300); mouse *anti*-FCV VP1 (Sc-80785, Santa Cruz Biotechnology) (1:500). Both antibodies were diluted in PBS and incubated overnight at 4ºC. Samples were washed three times with PBS for 5 min and incubated with the corresponding secondary antibodies: donkey anti-rabbit Alexa 488 and anti-mouse Alexa 594 (Invitrogen), (1:500), and incubated 1 h at RT. After three washes with PBS-1X, samples were incubated with 1 mg/ml of 4′6′-diamidino-2-phenylindole (DAPI) for 3 min. Samples were washed 3 times with PBS, mounted with 90% glycerol-PBS, and analyzed using a Zeiss LSM-700 confocal microscope.

Proximity ligation assay. Interactions between the p53 protein with FCV dsRNA, VP1, or NS6/7 proteins were detected by a Duo link In Situ-Fluorescence Kit (Sigma-Aldrich) in FCV-infected cells (MOI of 5) following the manufacturer instructions. Briefly, after the indicated hpi, cells were fixed and permeabilized in 0.5% Triton X100 for 20 min. After preincubation with a blocking agent for 1 h at RT, samples were incubated overnight with the following primary antibodies: rabbit *anti*-p53 (GTX50438; Gene Tex) and anti NS6/7 (kindly donated by I Goodfellow), and mouse *anti*-FCV VP1 in a 1:300 dilution, and *anti*-dsRNA MAB J2 *anti*-dsRNA (kindly donated by RM del Ángel) in a 1:200 dilution (Soto-Acosta, Bautista-Carbajal, Cervantes-Salazar, Angel-Ambrocio, & del Angel, 2017). Mock-infected cells incubated with both primary antibodies or FCV-infected cells incubated only with the *anti*-VP1 or the *anti*-p53 antibodies were included as negative controls.

***In silico* analysis of the protein-protein interactions.** The sequence of the *Felis catus* p53 and MDM2, as well as the GST proteins, were obtained from GeneBank (National Center of Biotechnology Information) sequence accession numbers: (BAA05653.1 NP_001009346.1; and XP_003994894.4) and their three-dimensional (3D) structure was predicted with the RaptorX software (http://raptorx.uchicago.edu/StructPredV2/predict/). The 3D crystal structure of FCV VP1 (PDB entry 3M8L) was taken from the protein data bank (PDB). Molecular docking simulations were predicted using the ClusPro protein-protein docking experiments server (https://cluspro.bu.edu/). The energies of the models obtained were compared with the predictions of interactions reported before as p53 with MDM2 (as positive control) and p53 with GST (negative control). All the binding energies were obtained by hydrophobic interaction models. Dockings were performed with the balance free-energy function, and the values were statistically analyzed and compared. The structures were represented using PyMOL software (PyMOL Molecular Graphics System, version 2.0; Schrödinger, LLC).

Statistical analysis. Statistical analyses were performed using the GraphPad Prism 8.4.0 software (CA, USA). Two-way analysis of variance (ANOVA) was used. Error bars represent the standard deviation from at least three independent experiments.

3. Results

p53 levels and subcellular localization does not change during FCV infection. It is widely known that viruses can modulate p53 steady-state by changing its expression, activity, localization, and by translational modifications [Reviewed in (Sato and Tsurumi, 2013) (Aloni-Grinstein et al., 2018)]. To determine if the levels or the subcellular localization of p53 were modified during FCV infection, the expression of p53 in mock-infected and infected CrFK cells were determined by western blotting and immunofluorescence assays (Figs. 1 and 2). Total protein extracts from mock-infected and infected cells at 0, 1, 3, 5, 7, 9, and 11 h were submitted to SDS-PAGE, and p53 relative expression was determined by western blotting. Similar levels of p53 were observed in both mock-infected and infected cells in all hpi analyzed (Fig. A1 and B1). However, the levels of p21, a gene downstream of p53, were found downregulated from 7 and up to 11 hpi, suggesting a modified transcriptional activity of p53 at late hpi (Fig A1 and C1).

The finding that p53 levels were similar during infection correlates with the immunofluorescence assays results where the fluorescence intensity of p53 was similar in both mock-infected and infected cells and in all the conditions tested (3, 5, and 7 hpi) (Fig. 2). Likewise, the localization of p53 was observed mainly in the cytoplasm in both mock-infected and infected cells (Fig. 2). In contrast, increasing amounts of NS6/7 and VP1 protein were observed from 3 hpi in both western blotting (Fig. 1A) and immunofluorescence assays (Supplementary Fig., and 1 Fig. 2A), indicating the progression of the infection (Figs. 1A and 2). One interesting finding was that Pearson correlation coefficient (PCC) between p53 and VP1 increases as the infection progresses, with values of 0.32 ± 0.19, 0.55 ± 0.19 at 3 and 5 hpi (Supplementary Fig. 1) and 0.65 ± 0.11 at 7hpi (Fig. 2A), suggesting that these two proteins may associate as the infection progresses.

p53 interacts with VP1 *in vitro* and in FCV infected cells. The colocalization results suggest that p53 and VP1 interact in FCV infected cells. To test this possibility, a glutathione-agarose pull-down assay was carried out using a FCV VP1-GST fusion protein. Purified recombinant FCV VP1-GST was bound to glutathione-agarose resin and incubated with CrFK mock-infected cell lysates and the interacting proteins analyzed by western blotting (Fig. 2B). Glutathione-agarose-VP1-GST but not glutathione-agarose GST was able to precipitate p53 present in cell lysates (Fig. 2B, left panel), strongly suggesting that both proteins interact. In agreement with these results, far-western blotting carried out using mock-infected, and FCV infected cells and the p53-His recombinant protein, resulted in the detection of several bands from 130 to 34 kDa in the infected cell extracts; two of them of 60 and 75 kDa, corresponding to the molecular weight of the mature FCV VP1 and its precursor respectively (Supplementary Fig. 2A). Similarly, when the assay was performed in the presence of the VP1-GST recombinant protein, several bands from 100 to 42 kDa were detected in both mock-infected and infected cell lysates; among them two bands of 53 and 42 kDa that correspond to the molecular weights of p53 and the FCV functional receptor fJAM-1 (Makino et al., 2006) respectively (Supplementary Fig. 2B).

To confirm the interaction between VP1 and p53 in infected cells, a proximity ligation assay (PLA) analysis was performed in FCV infected CrFK cells. The PLA allows the detection of protein-protein interactions while preserving the cell architecture, and the generated signal can be quantified. A positive signal (red dots) in the cytoplasm was detected in FCV infected cells at 5 (Supplementary Figs. 3) and 7 hpi (Fig. 2C)

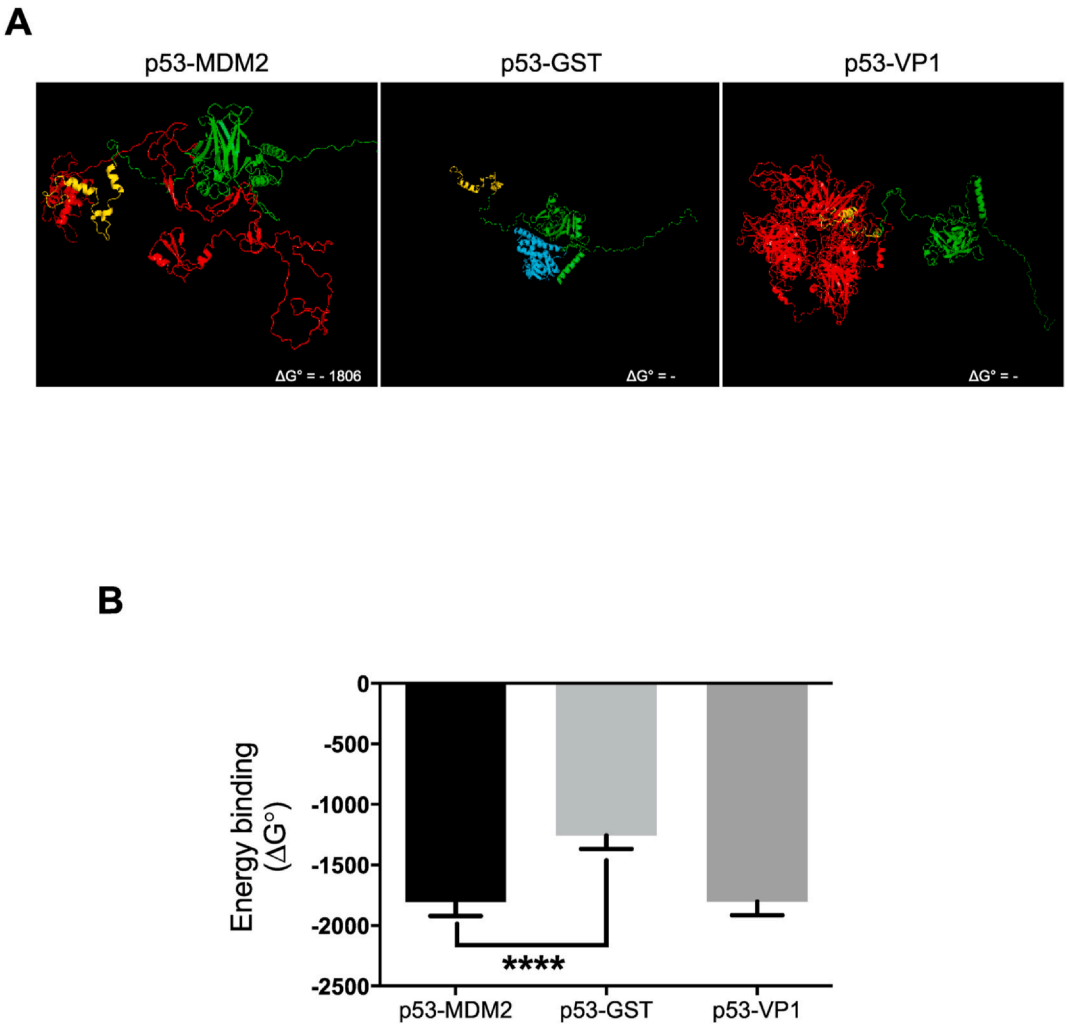

Fig. 3. *In silico* prediction of the interaction of FCV VP1 and p53. A) Interaction of p53 with MDM2 used as a positive control; p53 with GST as negative control; and P53 with FCV VP1 interaction. The *Felis catus* p53 model (green) was obtained from the RaptorX server. The p53 N-terminal region is indicated in yellow. B) Protein-protein binding energy (ΔG°) for each prediction was plotted, and values were estimated by ClusPro server (https://cluspro.bu.edu/home.php). Standard deviations were obtained from at least 3 independent assays. Values of $p \leq 0.0001$ (****), calculated by one-way ANOVA using GraphPad Prism 8.00 software, are indicated.

incubated with both *anti*-VP1 and *anti*-p53 antibodies, confirming that VP1 interacts with p53 in infected cells. No signal was detected in mock-infected cells incubated with both primary antibodies (Fig. 2C) or in infected cells incubated only with the *anti*-VP1 antibody (Supplementary Fig. 3A), demonstrating the specificity of the signal.

Modeling of molecular interactions between FCV VP1 and p53. The molecular interaction between FCV VP1 and p53 was also predicted by *in silico* analysis. A p53 constructed three-dimensional model was obtained using the RaptorX server (http://raptorx.uchicago.edu) (10.1093/bioinformatics/btt211), and a molecular docking predicted between p53 and VP1 using the ClusPro protein-protein docking (cluspro.org) was performed. A similar energy binding ΔG° (cal/mol) average calculated for VP1-p53 (ΔG° = -1802) interaction and p53-MDM2 (ΔG° = -1806), a well known interaction used as a positive control was obtained (Momand et al., 1992) (Chen et al., 1993), in contrast to the low energy binding of p53-GST (ΔG° = -1256) used as a negative control (Fig. 3), supporting the notion that p53 interacts with FCV VP1. Moreover, the *in vitro* interaction of VP1 and p53 was determined by an overlay assay. VP1-GST, GST, and p53-His (5 μg) were subjected to SDS-PAGE and transferred to a nitrocellulose membrane, and incubated with the recombinant p53-His followed by the anti-His antibody (Supplementary Fig. 4). A band of 95 kDa, corresponding to the molecular weight of VP1-GST, was observed (line 1), suggesting the interaction between these two proteins. The negative and positive controls are shown (Supplementary Fig. 4, lines 2, and 3).

p53 is recruited to the replicative complexes and interacts with the FCV dsRNA and the NS6/7 protease-polymerase protein. The replicative complexes (RC) are the membranous structures where the genomic and subgenomic viral RNA replication occur, and it is well known that the dsRNA and VP1 are two of the most abundant viral components in these perinuclear structures (Green et al., 2002). Since we have seen that much of the colocalization between p53 and VP1 is observed in the perinuclear area, we speculate if p53 could be recruited to the RC. Therefore, the colocalization of p53 and the viral dsRNA was determined by immunofluorescence assays using the *anti*-p53 (red) and *anti*-dsRNA (green) antibodies (Fig. 4). While the p53 signal was observed mainly in the cytoplasm of both mock-infected and infected cells at 3, 5, and 7 h, the dsRNA signal was only observed in the perinuclear area from the infected cells at 5 and 7hpi (Supplementary Fig. 5 and Fig. 4A). A colocalization between p53 and the dsRNA was observed in the perinuclear area, with a PCC 0.2 ± 0.03 and 0.50 ± 0.09 at 3 and 5 hpi respectively (Supplementary Fig. 5) and 0.59 ± 0.11 at 7 hpi (Fig. 4A), indicating that as the infection progresses p53 is recruited to the FCV RC and associates with the dsRNA.

To confirm the direct interaction between p53 and the dsRNA, a PLA analysis was performed in FCV infected CrFK cells. A positive

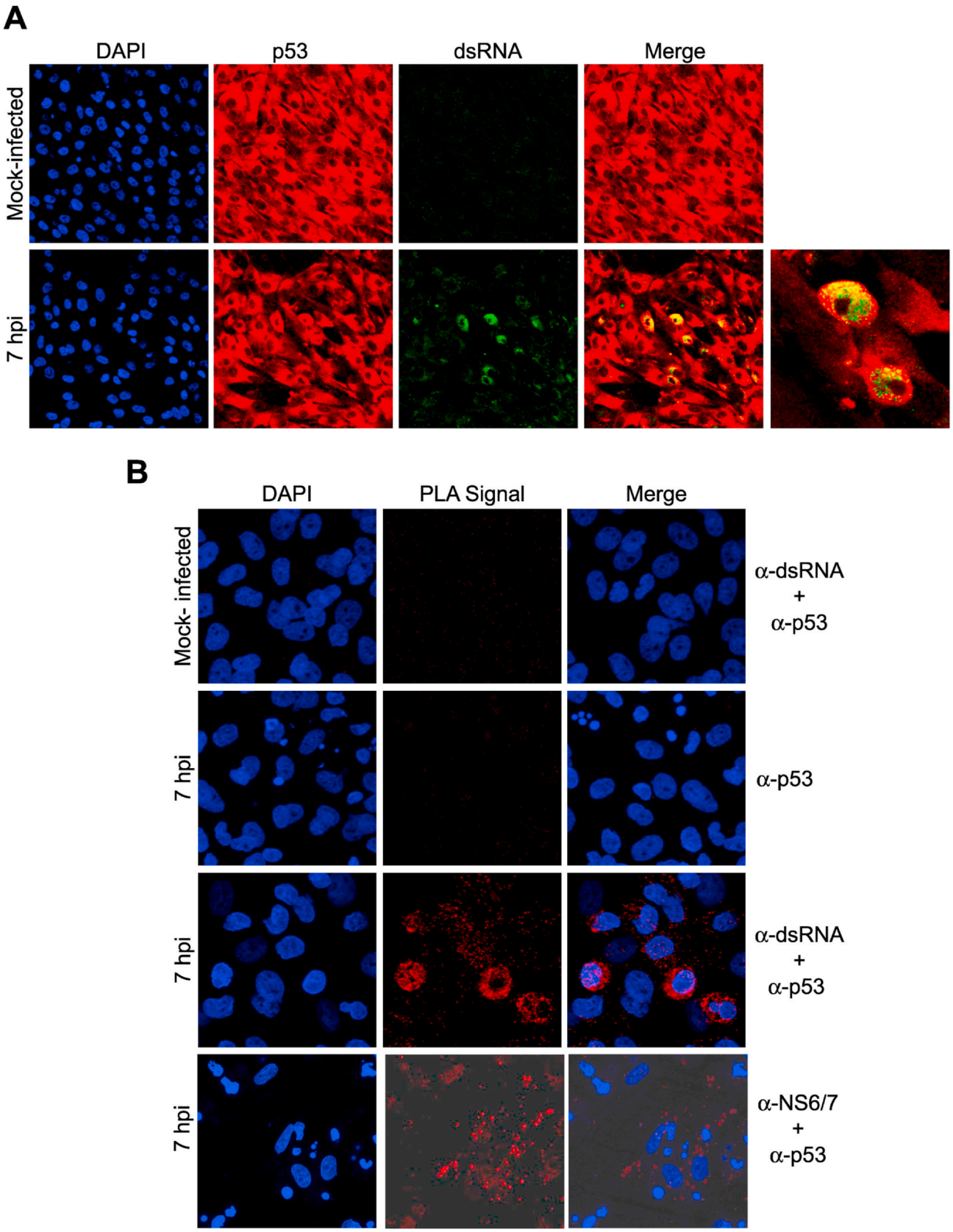

Fig. 4. p53 interact with the dsRNA and the NS6/7 protein during FCV infection. A) Monolayers of mock-infected or FCV CrFK cells were infected at an MOI of 5 at 7 h, and immunostained with an *anti*-p53 (red), and *anti*-dsRNA (green) antibodies, followed by Alexa Fluor 594 (red) and Alexa Fluor 488 (green) respectively. DAPI was used for nuclear (blue) staining. The cells were examined in a Zeiss LSM 700 confocal microscope. Images correspond to a z-stack of 15 slices and are representative of three independent experiments. Merged and zoom images are indicated. Colocalization rates of p53 and dsRNA at 7hpi (0.59 ± 0.11) were calculated by Pearson's coefficient correlation using the Icy software (http://icy.bioimageanalysis.org). B) Proximity ligation assay (PLA-Duolink) between the dsRNA and p53 and NS6/7 and p53 in FCV infected cells at 7 h. PLA signals (red) represent dual-recognition PLA against p53 and VP1. DAPI was used for nuclear (blue) staining. The cells were examined in a Zeiss LSM 700 confocal microscope.

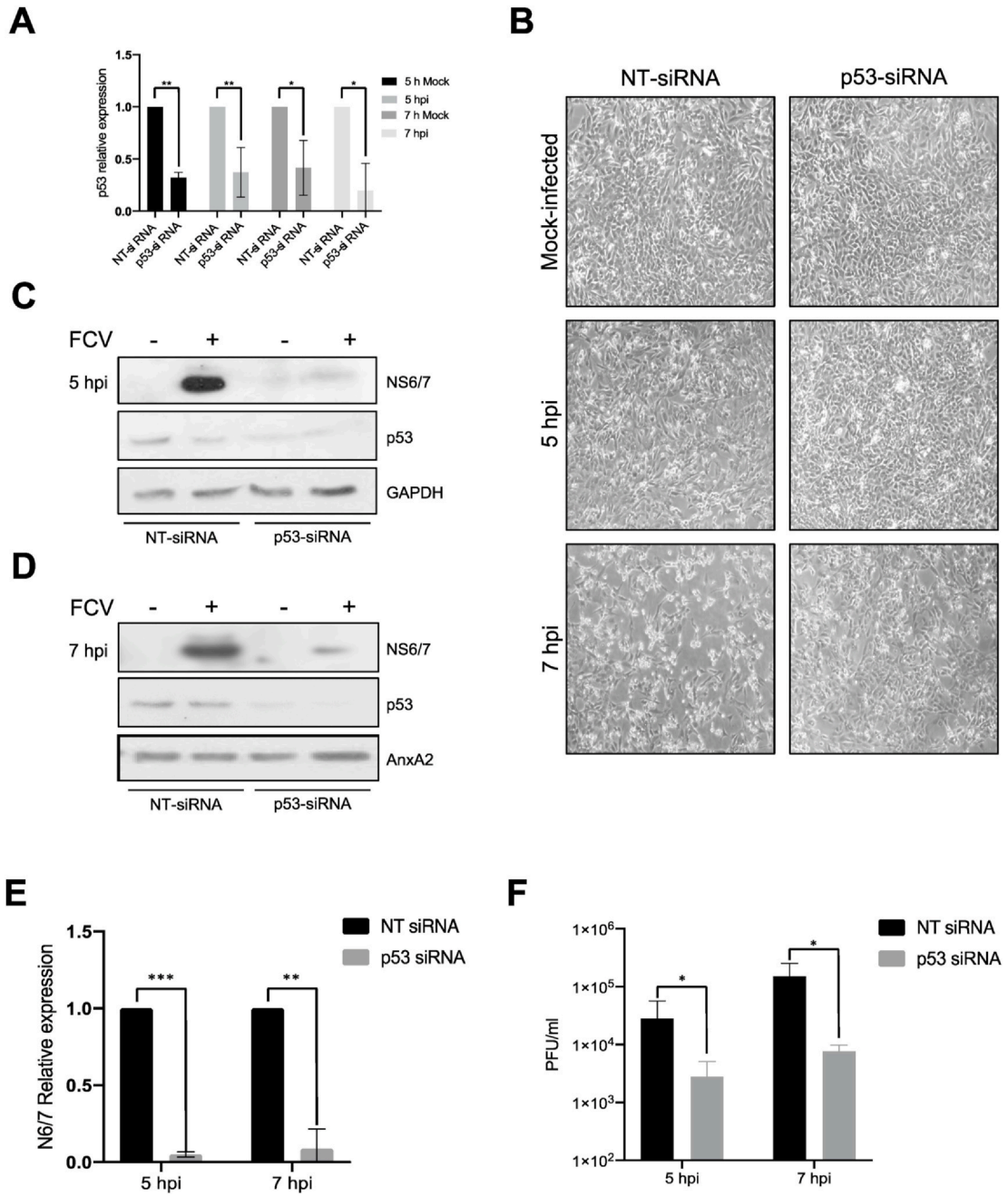

Fig. 5. p53 is implicated in an efficient FCV replication. CrFK cells were transfected with a non-targeting (NT)-siRNA or a siRNAs specific for p53 (p53-siRNA) for 24 h, and mock-infected or infected with FCV at an MOI 5 for 5 and 7 h. A) The CPE was evaluated by light microscopy. Total protein extracts were obtained at B) 5 and C) 7 hpi and subjected to SDS-PAGE. Protein expression was analyzed by western blotting using specific antibodies. NS6/7 indicates virus infection; GAPDH and AnxA2 were used as the loading controls. D) p53 and E) NS6/7 band intensities of scanned images were quantified using ImageJ software and expressed as relative expression. Standard deviations were obtained from at least 3 independent assays. Values of $p \leq 0.05$ (**) and $p \leq 0.0001$ (***), calculated by two-way ANOVA using GraphPad Prism 8.00 software are indicated. F) Virus particles were obtained at 5 and 7 hpi and assessed by plaque assay. Standard deviations were obtained from at least 3 independent assays. Values of $p \leq 0.05$ (*), calculated by *t*-test using GraphPad Prism 8.00 software are indicated.

signal (red dots) in the cytoplasm was detected in FCV infected cells at 7 hpi stained with both *anti*-p53 and *anti*-dsRNA antibodies, strongly suggesting that p53 interacts with the dsRNA in the FCV RC at this time post-infection (Fig. 4B). Moreover, the interaction of p53 with other components of the RC, the NS6/7 protein was also detected (Fig. 4B), confirming that p53 is recruited in the RC. No signal was detected in mock-infected cells incubated with both primary antibodies or in infected cells incubated with the *anti*-p53 antibody alone, demonstrating the specificity of the signal (Fig. 4B and Supplementary Fig. 6).

The reduction of p53 expression resulted in a delay of the cytopathic effect, and a reduction in the viral protein production and FCV replication. To evaluate if p53 plays a role on FCV replication, CrFK cell monolayers were transfected with NT-siRNA or p53-siRNA for 24 h and infected with FCV at an MOI of 5. After 5 and 7 h, the cytopathic effect (CPE), the levels of viral protein and virus progeny production were analyzed (Fig. 5). A delay in the CPE of cells transfected with the p53-siRNA at 5 and more evident at 7hpi, was observed when compared to the CPE from the non-targeting-siRNA treated infected cells (Fig. 5B). This observation correlates with a 95 and 91% reduction in the NS6/7 viral protein levels at 5 and 7 hpi compared to

the levels of NS6/7 in cells transfected with the non-targeting siRNA (Fig. 5C–E). This reduction in viral protein observed in the p53 siRNA-transfected cells was not the consequence of a reduction of cell viability or cell proliferation (Supplementary Figs. 7A and 7B) or any gross effects on the host protein synthesis since the levels of glyceraldehyde-3-phosphate dehydrogenase (GAPDH) or AnxA2 were unaffected (Fig. 5C and D). A 60% decrease in p53 levels in transfected CrFK cells with specific siRNAs in comparison to the levels from cells transfected with the non-targeting (NT) siRNA was obtained by band quantification using the ImageJ software (Fig. 5A).

Due to the reduction of viral proteins as a result of p53 knockdown, virus production was evaluated by plaque assays. p53 knockdown resulted in a 90.2 and 95% reduction in the FCV progeny production at 5 and 7hpi, respectively (Fig. 5F), indicating that p53 is required for FCV replication.

4. Discussion

p53 is a tumor suppressor that can be accumulated and activated by varied stress signals; once activated, this protein regulates cellular pathways that define the cell fate, such as cell cycle arrest, cell differentiation, cell senescence, and apoptosis cell death [Reviewed in: (Aloni-Grinstein et al., 2018)]. The main function of p53 is to preserve the homeostasis by direct or indirect activation or repression of a large set of genes [Reviewed in: (Grossi et al., 2016)]. One of the most important proteins activated by p53, is the CDK inhibitor p21 that regulates cell pathways involved in the cell cycle arrest and apoptosis (Karimian et al., 2016); therefore, its expression is an indicator of the p53 transcription activity (Georgakilas et al., 2017). Notwithstanding, p53 can also control other pathways such as autophagy, metabolism, cell pluripotency, and plasticity, and facilitates an iron-dependent form of cell death known as ferroptosis (Kastenhuber and Lowe, 2017). To regulate its steady-state, p53 is labeled by the MDM2 ubiquitin ligase for its proteasomal ubiquitin-dependent pathway degradation in unstressed cells, where p53 levels are to low to be detected (Levine and Oren, 2009). Upon cell stress as DNA damage, p53 is phosphorylated and evade the proteasomal degradation; then it is stabilized and activated as a transcription factor, leading to cell cycle arrest or apoptosis induction by p53-mediated gene expression cascades. Therefore, the cell pathways linked to p53 dynamics are mediated by its expression levels and its post-translational modifications [Reviewed in: (Sato and Tsurumi, 2013).

Upon viral infections, the p53 steady-state can be modified as a result of cell stress and favors an efficient replicative cycle. As widely reported, some viruses can activate p53; some others induce its inhibition and/or degradation, and some more can modulate both its activation and degradation at specific stages of the infection [Reviewed in: (Aloni-Grinstein et al., 2018)]. Even though it is well known that all the members of the *Caliciviridae* family induce apoptosis, the role of p53 in this pathway or in other stages of viral replication has not been studied; therefore, the aim of this work was to determine if p53 host cell protein has a role in the replicative cycle of FCV, one of the best models to study the replication of this family.

During FCV infection, p53 expression levels remained unchanged, and its subcellular localization was mostly in the cytoplasm in both mock-infected and infected cells. However, its transcription activity was modified during infection; as the relative expression of the cyclin-dependent kinase inhibitor p21 one of the targets of p53 activity was reduced from 7 and up to 11 hpi with FCV. This result correlates with the fact that inhibition of apoptosis is a function of p21 [Reviewed in: (Gartel and Tyner, 2002)].

The colocalization between p53 and the FCV VP1 observed form 3hpi, and that increased at later times post-infection was observed, suggest that both proteins interact from the early stages of infection. To this regard, during Influenza A virus (IAV) infection, p53 is activated in a biphasic pattern: in the early stages and later, at the middle-late phase of infection, during the apoptotic onset (Shen et al., 2009) (Turpin et al., 2005) (Xue Wang et al., 2014). While IAV protein NS1 a non-essential virulence factor, interacts with p53 inhibiting its transcriptional activity and apoptosis (Xiaodu Wang et al., 2010b); the IAV nucleoprotein (NP), with multiple roles such as the viral RNA transcription, replication, and packaging (Portela and Digard, 2002), interacts with p53, increasing its transcriptional activity (Xiaodu Wang et al., 2012), and modulating the immune response (B. Wang et al., 2018).

Therefore, we first wanted to determine if p53 interacted with FCV VP1. The *in vitro* association of both p53 and VP1 was suggested by molecular docking *in silico* analysis as well as by far-western blotting and further corroborated by pull-down and overlay assays. Moreover, the interaction between p53 and VP1 was confirmed in infected cells by PLA assays.

Regulation of p53 is also the result of the interaction of viral capsid proteins with MDM2, its main regulatory protein. The C-terminus of the of the ZIKV capsid protein interacts with MDM2, activating the death of infected neural cells (Teng et al., 2017); while the capsid protein of the WNV interacts with the human double minute-2 (HDM2), which is sequestered into the nucleolus with the resulting stabilization of p53 and apoptosis induction (Yang et al., 2008). If MDM2 homolog in CrFK cells interacts with any FCV protein or if it is modified during infection remains to be determined.

Taking into account that VP1 is the most abundant protein in the RCs (Green et al., 2002), it was likely that p53 was recruited in these membranous structures. The colocalization of p53 with the dsRNA in the perinuclear region showed by immunofluorescence assays, and the interaction of both molecules demonstrated by PLA assays strongly suggests that p53 is present in the RCs; therefore, the association between VP1 and p53 could be taking place in these cellular compartments. Furthermore, the association of p53 with the protease-polymerase NS6/7 protein by PLA corroborates the presence of p53 in the RCs.

Considering that p53 is associated with three FCV components, we hypothesized that it might have a role for efficient viral replication. The role of p53 in the FCV replication was demonstrated by knocking down its expression with specific p53-siRNAs. Even though p53 is an abundant protein, the cells treated with the specific p53-siRNAs showed at least a 60% reduction of these protein levels, which caused a delay in the cytopathic effect of the FCV-infected cells, when compared to the infected cells treated with the non-targeting siRNA. This delay in the cytopathic effect correlates with a strong reduction of the NS6/7 viral protein expression at 5 and 7hpi and a 1log reduction in the viral progeny production, indicating that p53 participates for an efficient FCV replication, a role that is for the first time reported for a member of the *Caliciviridae* family.

Taken into account that p53 is recruited in the RC, where replication of both gRNA and sgRNAs, as well as VP1 translation, occur and that p53 is associated with VP1, NS6/7, and with the dsRNA, it could be possible that p53 participates in these viral processes. On the one hand, RNA-linked p53 has been reported to be a major biological active form of p53 (Samad and Carroll, 1991). p53 in the cytoplasm exerts high levels of 3′ to 5′ exoribonuclease activity on ss-DNA, ds-DNA, ss-RNA, ds-RNA, and RNA/DNA substrates (Derech-haim, Friedman, Hizi and Bakhanashvili, 2020) (Grinberg et al., 2010). Some RNA viruses such as coronaviruses, toroviruses, and roniviruses encode for 3' to 5′exoribonucleases that are critically involved in the synthesis of multiple RNAs from its large genomic RNA templates and performs a proofreading function required for high-fidelity replication (Minskaia et al., 2006). Moreover, the human immunodeficiency virus (HIV)-1, which has a small RNA genome, the cytoplasmic p53 increases the accuracy of DNA synthesis by the reverse transcriptase (RT) (Bakhanashvili et al., 2004). Thus, it is possible that p53 may play a role for an efficient FCV RNA replication. On the other hand, the low levels of NS proteins when p53 was knocked down could be the result of an inefficient translation or

reduced levels of the gRNA. In this regard, since VP1 is also present in the RC and associated with p53, and the RdRp NS6/7 is associated with p53, it is possible that p53 through its interaction with VP1 contributes to the RdRp activity, as during norovirus replication (Subba-Reddy et al., 2011). Interestingly, p53 can direct either the complete degradation of and decrease in the level of cellular dsRNA, or incomplete dsRNA degradation that results in the generation of short dsRNA products (Grinberg et al., 2010). It would be interesting to determine if p53 could participate in the generation of the FCV gRNA or sgRNA. p53 can be extensively posttranslationally modified in response to various types of cellular stress that are implicated in the regulation of its levels, as well as its DNA binding and transcriptional activities. Since modifications in p53 are implicated in the induction or repression of a variety of its target genes, it is possible that this protein can have other functions during infection.

Here we have shown that p53 is associated with FCV elements present in the RC, such as the dsRNA; however, the specific role of this interaction is not yet known. p53 acts as a transcription factor by binding to some response elements (p53RE) within the genomic DNA (B. Wang, et al., 2010). Moreover, p53 also interacts with the genomes of double-stranded DNA viruses. p53 binds to a consensus p53 binding sequence within the non-coding region of the Human papillomavirus 77 (HPV77) genome and activates its activity in response to UV radiation (Purdie et al., 1999). More recently, two novel functional p53 responsive elements (RE) have been identified in the HSV-1 genome, modulating the expression of viral proteins that may determine the progression of the lytic phase or the establishment of latency (Hsieh et al., 2014). Hepatitis B virus (HBV) transcription and replication are repressed by p53 sequence-specific binding to an enhancer element within its genome. This transcriptional effect of p53, when bound to this viral DNA region, can be modulated by adjacent enhancer elements as well as with interactions with other DNA-proteins (Ori et al., 1998). p53 can also bind to the long terminal repeat of the HIV-1 that mediates mutant p53 transactivation (Gualberto et al., 1995). An interesting finding was that different conformations of p53 recognize different DNA binding sites and mediate distinct biological functions.

Although p53 has been typically considered a sequence-specific DNA-binding transcription factor, its interaction with different cellular RNAs has been described in a variety of contexts [Reviewed in: (Riley and Maher, 2007)]. p53 binds to the 5′-UTR of its own mRNA (Mosner et al., 1995); to the 5.8s ribosomal RNA (rRNA), and to the CDK4 and the fibroblast growth factor 2 (FGF-2) mRNA [Reviewed in: (Riley and Maher, 2007)]. Although p53-RNA interactions are mediated by its nucleic-acid-binding domain responsible for DNA recognition, they are most probably sequence nonspecific [Reviewed in: (Riley and Maher, 2007)]. However, no reports regarding the interaction of p53 with a viral RNA have been previously described. Here we found that p53 interacts with three components of the FCV RC: VP1, NS6/7, and the dsRNA. The knockdown of p53 caused a significant reduction of viral protein synthesis and virus yield, indicating its role for an efficient viral replication. Future studies will provide further insights into the specific mechanism of action of p53 in FCV replication.

Credit author statement

ATU generate the experimental data. ATU and ALGE collaborated equally in the manuscript writing. ALGE coordinated and edited the manuscript.

Acknowledgments

We thank Romel Rosales, José Humberto Pérez-Olais, Rosa M. del Ángel, and Juan Ludert for many helpful suggestions and critical comments on the manuscript. We also thank Clotilde Cancio-Lonches and Yoloxochitl Paredes-Morales for technical assistance.This work was supported by grant 0250696 from Consejo Nacional de Ciencia y Tecnología (Conacyt).

Appendix A. Supplementary data

Supplementary data to this article can be found online at https://doi.org/10.1016/j.virol.2020.08.008.

References

Aloni-Grinstein, R., Charni-Natan, M., Solomon, H., Rotter, V., Aloni-Grinstein, R., Charni-Natan, M., et al., 2018. p53 and the viral connection: back into the future ‡. Cancers 10 (6), 178. https://doi.org/10.3390/cancers10060178.

Bailey, D., Kaiser, W.J., Hollinshead, M., Moffat, K., Chaudhry, Y., Wileman, T., Goodfellow, I.G., 2010. Feline calicivirus p32, p39 and p30 proteins localize to the endoplasmic reticulum to initiate replication complex formation. J. Gen. Virol. 91 (3), 739–749. https://doi.org/10.1099/vir.0.016279-0.

Bakhanashvili, M., Novitsky, E., Lilling, G., Rahav, G., 2004. P53 in cytoplasm may enhance the accuracy of DNA synthesis by human immunodeficiency virus type 1 reverse transcriptase. Oncogene 23 (41), 6890–6899. https://doi.org/10.1038/sj.onc.1207846.

Barrera-Vázquez, O.S., Cancio-Lonches, C., Hernández-González, O., Chávez-Munguia, B., Villegas-Sepúlveda, N., Gutiérrez-Escolano, A.L., 2019. The feline calicivirus leader of the capsid protein causes survivin and XIAP downregulation and apoptosis. Virol. 527, 146–158. https://doi.org/10.1016/j.virol.2018.11.017.

Cancio-Lonches, C., Yocupicio-Monroy, M., Sandoval-Jaime, C., Galvan-Mendoza, I., Urena, L., Vashist, S., Gutierrez-Escolano, A.L., 2011. Nucleolin interacts with the feline calicivirus 3' untranslated region and the protease-polymerase NS6 and NS7 proteins, playing a role in virus replication. J. Virol. 85 (16), 8056–8068. https://doi.org/10.1128/jvi.01878-10.

Chen, J., Marechal, V., Levine, A.J., 1993. Mapping of the p53 and mdm-2 interaction domains. Mol. Cell Biol. 13 (7), 4107–4114. https://doi.org/10.1128/mcb.13.7.4107.

Crandell, R.A., Fabricant, C.G., Nelson-Rees, W.A., 1973. Development, characterization, and viral susceptibility of a feline (Felis catus) renal cell line (CRFK). *In* Vitro 9 (3), 176–185. https://doi.org/10.1007/BF02618435.

Derech-haim, S., Friedman, Y., Hizi, A., Bakhanashvili, M., 2020. p53 Regulates its Own Expression by an Intrinsic Exoribonuclease Activity through AU-Rich Elements, vol. 2.

El Ghouzzi, V., Bianchi, F.T., Molineris, I., Mounce, B.C., Berto, G.E., Rak, M., et al., 2016. ZIKA virus elicits P53 activation and genotoxic stress in human neural progenitors similar to mutations involved in severe forms of genetic microcephaly and p53. Cell Death Dis. 7 (10). https://doi.org/10.1038/cddis.2016.266.

Emmott, E., Sorgeloos, F., Caddy, S.L., Vashist, S., Sosnovtsev, S., Lloyd, R., et al., 2017. Norovirus-mediated modification of the translational landscape via virus and host-induced cleavage of translation initiation factors. Mol. Cell. Proteomics 16 (4), S215–S229. https://doi.org/10.1074/mcp.M116.062448.

Escobar-Herrera, J., Medina-Ramírez, F.J., Gutiérrez-Escolano, A.L., 2007. A carboxymethyl-cellulose plaque assay for feline calicivirus. J. Virol Methods 146 (1–2), 393–396. https://doi.org/10.1016/J.JVIROMET.2007.07.013.

Gartel, A.L., Tyner, A.L., 2002. The role of the cyclin-dependent kinase inhibitor p21 in apoptosis. Mol. Canc. Therapeut. 1 (8), 639–649.

Georgakilas, A.G., Martin, O.A., Bonner, W.M., 2017. p21: a two-faced genome guardian. Trends Mol. Med. 23 (4), 310–319. https://doi.org/10.1016/j.molmed.2017.02.001.

Green, K.Y., Mory, A., Fogg, M.H., Weisberg, A., Belliot, G., Wagner, M., et al., 2002. Isolation of enzymatically active replication complexes from feline calicivirus-infected cells. J. Virol. 76 (17), 8582–8595. https://doi.org/10.1128/jvi.76.17.8582-8595.2002.

Grinberg, S., Teiblum, G., Rahav, G., Bakhanashvili, M., 2010. p53 in cytoplasm exerts 3′→5′ exonuclease activity with dsRNA. Cell Cycle 9 (12), 2442–2455. https://doi.org/10.4161/cc.9.12.12053.

Grossi, E., Sánchez, Y., Huarte, M., 2016. Expanding the p53 regulatory network: LncRNAs take up the challenge. Biochimica et Biophysica Acta - Gene Regulatory Mechanisms 1859 (1), 200–208. https://doi.org/10.1016/j.bbagrm.2015.07.011.

Gualberto, A., Hixon, M.L., Finco, T.S., Perkins, N.D., Nabel, G.J., Baldwin, A.S., 1995. A proliferative p53-responsive element mediates tumor necrosis factor alpha induction of the human immunodeficiency virus type 1 long terminal repeat. Mol. Cell Biol. 15 (6), 3450–3459. https://doi.org/10.1128/mcb.15.6.3450.

Herbert, T.P., Brierley, I., Brown, T.D.K., 1996. Detection of the ORF3 polypeptide of feline calicivirus in infected cells and evidence for its expression from a single, functionally bicistronic, subgenomic mRNA. J. Gen. Virol. 77 (1), 123–127. https://doi.org/10.1099/0022-1317-77-1-123.

Hsieh, J.C., Kuta, R., Armour, C.R., Boehmer, P.E., 2014. Identification of two novel functional p53 responsive elements in the herpes simplex virus-1 genome. Virology 460–461 (1), 45–54. https://doi.org/10.1016/j.virol.2014.04.019.

Karimian, A., Ahmadi, Y., Yousefi, B., 2016. Multiple functions of p21 in cell cycle, apoptosis and transcriptional regulation after DNA damage. DNA Repair 42, 63–71. https://doi.org/10.1016/j.dnarep.2016.04.008.

Kastenhuber, E.R., Lowe, S.W., 2017. Putting p53 in context. Cell 170 (6), 1062–1078. https://doi.org/10.1016/j.cell.2017.08.028.

Levine, A.J., Oren, M., 2009. The first 30 years of p53: growing ever more complex. Nat. Rev. Canc. 9 (10), 749–758. https://doi.org/10.1038/nrc2723.

Ma-Lauer, Y., Carbajo-Lozoya, J., Hein, M.Y., Müller, M.A., Deng, W., Lei, J., et al., 2016. P53 down-regulates SARS coronavirus replication and is targeted by the SARS-unique

domain and PLpro via E3 ubiquitin ligase RCHY1. Proceedings of the National Academy of Sciences of the United States of America 113 (35), E5192–E5201. https://doi.org/10.1073/pnas.1603435113.

Makino, A., Shimojima, M., Miyazawa, T., Kato, K., Tohya, Y., Akashi, H., 2006. Junctional adhesion molecule 1 is a functional receptor for feline calicivirus. J. Virol. 80 (9), 4482–4490. https://doi.org/10.1128/JVI.80.9.4482-4490.2006. LP –.

Minskaia, E., Hertzig, T., Gorbalenya, A.E., Campanacci, V., Cambillau, C., Canard, B., Ziebuhr, J., 2006. Discovery of an RNA virus 3′→5′ exoribonuclease that is critically involved in coronavirus RNA synthesis. Proc. Nat. Academy of Sci. U.S.A. 103 (13), 5108–5113. https://doi.org/10.1073/pnas.0508200103.

Mishra, P.A., Laboratories, U., 2015. p53: An overview. (January 2013).

Momand, J., Zambetti, G.P., Olson, D.C., George, D., Levine, A.J., 1992. The mdm-2 oncogene product forms a complex with the p53 protein and inhibits p53-mediated transactivation. Cell 69 (7), 1237–1245. https://doi.org/10.1016/0092-8674(92)90644-R.

Mosner, J., Mummenbrauer, T., Bauer, C., Sczakiel, G., Grosse, F., Deppert, W., 1995. Negative feedback regulation of wild-type p53 biosynthesis. EMBO J. 14 (18), 4442–4449. https://doi.org/10.1002/j.1460-2075.1995.tb00123.x.

Ori, A., Zauberman, A., Doitsh, G., Paran, N., Oren, M., Shaul, Y., 1998. p53 binds and represses the HBV enhancer: an adjacent enhancer element can reverse the transcription effect of p53. EMBO J. 17 (2), 544–553. https://doi.org/10.1093/emboj/17.2.544.

Peñaflor-téllez, Y., Trujillo-uscanga, A., Escobar-almazán, J.A., Gutiérrez-escolano, A.L., 2019. Immune response modulation by caliciviruses. 10(October), 1–14. https://doi.org/10.3389/fimmu.2019.02334.

Portela, A., Digard, P., 2002. The influenza virus nucleoprotein: a multifunctional RNA-binding protein pivotal to virus replication. J. Gen. Virol. 83 (4), 723–734. https://doi.org/10.1099/0022-1317-83-4-723.

Purdie, K.J., Pennington, J., Proby, C.M., Khalaf, S., De Villiers, E.M., Leigh, I.M., Storey, A., 1999. The promoter of a novel human papillomavirus (HPV77) associated with skin cancer displays UV responsiveness, which is mediated through a consensus p53 binding sequence. EMBO J. 18 (19), 5359–5369. https://doi.org/10.1093/emboj/18.19.5359.

Riley, K.J.L., Maher, L.J., 2007. p53-RNA interactions: new clues in an old mystery. RNA 13 (11), 1825–1833. https://doi.org/10.1261/rna.673407.

Saha, T., Kar, R.K., Sa, G., 2015. Structural and sequential context of p53: a review of experimental and theoretical evidence. Prog. Biophys. Mol. Biol. 117 (2–3), 250–263. https://doi.org/10.1016/j.pbiomolbio.2014.12.002.

Samad, A., Carroll, R.B., 1991. The tumor suppressor p53 is bound to RNA by a stable covalent linkage. Mol. Cell Biol. 11 (3), 1598–1606. https://doi.org/10.1128/mcb.11.3.1598.

Santos-Valencia, J.C., Cancio-Lonches, C., Trujillo-Uscanga, A., Alvarado-Hernández, B., Lagunes-Guillén, A., Gutiérrez-Escolano, A.L., 2019. Annexin A2 associates to feline calicivirus RNA in the replication complexes from infected cells and participates in an efficient viral replication. Virus Res. 261, 1–8. https://doi.org/10.1016/J.VIRUSRES.2018.12.003.

Sato, Y., Tsurumi, T., 2013. Genome guardian p53 and viral infections. Rev. Med. Virol. 23 (4), 213–220. https://doi.org/10.1002/rmv.1738.

Shen, Y., Wang, X., Guo, L., Qiu, Y., Li, X., Yu, H., et al., 2009. Influenza A virus induces p53 accumulation in a biphasic pattern. Biochem. Biophys. Res. Commun. 382 (2), 331–335. https://doi.org/10.1016/J.BBRC.2009.03.018.

Sosnovtsev, Stanislav, Green, K.Y., 1995. RNA transcripts derived from a cloned full-length copy of the feline calicivirus genome do not require VpG for infectivity. Virology 210 (2), 383–390. https://doi.org/10.1006/VIRO.1995.1354.

Sosnovtsev, S.V., Belliot, G., Chang, K.-O., Onwudiwe, O., Green, K.Y., 2005. Feline calicivirus VP2 is essential for the production of infectious virions. J. Virol. 79 (7), 4012–4024. https://doi.org/10.1128/jvi.79.7.4012-4024.2005.

Sosnovtsev, Stanislav V., Prikhod'ko, E.A., Belliot, G., Cohen, J.I., Green, K.Y., 2003. Feline calicivirus replication induces apoptosis in cultured cells. Virus Res. 94 (1), 1–10. https://doi.org/10.1016/S0168-1702(03)00115-1.

Soto-Acosta, R., Bautista-Carbajal, P., Cervantes-Salazar, M., Angel-Ambrocio, A.H., del Angel, R.M., 2017. DENV up-regulates the HMG-CoA reductase activity through the impairment of AMPK phosphorylation: a potential antiviral target. PLoS Pathog. 13 (4). https://doi.org/10.1371/journal.ppat.1006257.

Stuart, A.D., Brown, T.D.K., 2006. Entry of feline calicivirus is dependent on clathrin-mediated endocytosis and acidification in endosomes. J. Virol. 80 (15), 7500–7509. https://doi.org/10.1128/jvi.02452-05.

Subba-Reddy, C.V., Goodfellow, I., Kao, C.C., 2011. VPg-primed RNA synthesis of norovirus RNA-dependent RNA polymerases by using a novel cell-based assay. J. Virol. 85 (24), 13027–13037. https://doi.org/10.1128/jvi.06191-11.

Teng, Y., Liu, S., Guo, X., Liu, S., Jin, Y., He, T., et al., 2017. An integrative analysis reveals a central role of P53 activation via MDM2 in Zika virus infection induced cell death. Frontiers in Cellular and Infection Microbiology 7 (JUL), 1–12. https://doi.org/10.3389/fcimb.2017.00327.

Turpin, E., Luke, K., Jones, J., Tumpey, T., Konan, K., Schultz-Cherry, S., 2005. Influenza virus infection increases p53 activity: role of p53 in cell death and viral replication. J. Virol. 79 (14), 8802–8811. https://doi.org/10.1128/jvi.79.14.8802-8811.2005.

Vinjé, J., Estes, M.K., Esteves, P., Green, K.Y., Katayama, K., Knowles, N.J., et al., 2019. ICTV virus taxonomy profile: Caliciviridae. J. Gen. Virol. 1469–1470. https://doi.org/10.1099/jgv.0.001332.

Wang, B., Lam, T.H., Soh, M.K., Ye, Z., Chen, J., Ren, E.C., 2018. Influenza A virus facilitates its infectivity by activating p53 to inhibit the expression of interferon-induced transmembrane proteins. Front. Immunol. 9 (MAY). https://doi.org/10.3389/fimmu.2018.01193.

Wang, B., Xiao, Z., Ko, H.L., Ren, E.C., 2010a. The p53 response element and transcriptional repression. Cell Cycle 9 (5), 870–879. https://doi.org/10.4161/cc.9.5.10825.

Wang, Xiaodu, Deng, X., Yan, W., Zhu, Z., Shen, Y., Qiu, Y., et al., 2012. Stabilization of p53 in influenza A virus-infected cells is associated with compromised MDM2-mediated ubiquitination of p53. J. Biol. Chem. 287 (22), 18366–18375. https://doi.org/10.1074/JBC.M111.335422.

Wang, Xiaodu, Shen, Y., Qiu, Y., Shi, Z., Shao, D., Chen, P., et al., 2010b. The non-structural (NS1) protein of influenza A virus associates with p53 and inhibits p53-mediated transcriptional activity and apoptosis. Biochem. Biophys. Res. Commun. 395 (1), 141–145. https://doi.org/10.1016/J.BBRC.2010.03.160.

Wang, Xue, Tan, J., Zoueva, O., Zhao, J., Ye, Z., Hewlett, I., 2014. Novel pandemic influenza A (H1N1) virus infection modulates apoptotic pathways that impact its replication in A549 cells. Microb. Infect. 16 (3), 178–186. https://doi.org/10.1016/j.micinf.2013.11.003.

Yang, M.R., Lee, S.R., Oh, W., Lee, E.W., Yeh, J.Y., Nah, J.J., et al., 2008. West Nile virus capsid protein induces p53-mediated apoptosis via the sequestration of HDM2 to the nucleolus. Cell Microbiol. 10 (1), 165–176. https://doi.org/10.1111/j.1462-5822.2007.01027.x.

Yuan, L., Chen, Z., Song, S., Wang, S., Tian, C., Xing, G., et al., 2015. P53 degradation by a coronavirus papain-like protease suppresses type I interferon signaling. J. Biol. Chem. 290 (5), 3172–3182. https://doi.org/10.1074/jbc.M114.619890.